Supporting Information

Identification of Small Molecule Inhibitors of RNase L by Fragment-Based Drug Discovery

Jinle Tang[1#], Beihua Dong[2#], Ming Liu[1], Shuyan Liu[3], Xiaogang Niu[4], Christina Gaughan[2], Abhishek Asthana[2], Huan Zhou[5], Zhengshuang Xu[1], Guoliang Zhang[3], Robert H. Silverman[2*], Hao Huang[1*]

[1]State Key Laboratory of Chemical Oncogenomics, Laboratory of Structural Biology and Drug Discovery， School of Chemical Biology and Biotechnology, Peking University Shenzhen Graduate School, Shenzhen 518055, China

[2]Department of Cancer Biology, Lerner Research Institute, Cleveland Clinic, Cleveland, OH 44195, USA

[3]National Clinical Research Center for Infectious Diseases, Shenzhen Third People's Hospital, Southern University of Science and Technology, Shenzhen 518112, China

[4]College of Chemistry and Molecular Engineering, Beijing Nuclear Magnetic Resonance Center, Peking University, Beijing 100871, China

[5]Shanghai Advanced Research Institute, Chinese Academy of Sciences, Shanghai 201214, China.

# These authors contributed equally to this work.

*To whom correspondence should be addressed:

E-mail:

Hao Huang - (Email: huang.hao@pku.edu.cn)

Robert H. Silverman - (Email: SILVERR@ccf.org)

Table of Contents

Table S1. Inhibition constants (IC_{50}) and ligand efficiencies (LE) of fragments identified in activity-based screening against human (H-) and porcine (P-) RNase L proteins.

NO.	Fragment	2D-structure	IC_{50}（μM） H-RNase L	LE H-RNase L	IC_{50} (μM） P-RNase L	LE P-RNase L
1	CC39814	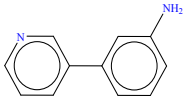	202	0.40	405	0.37
2	KM05073	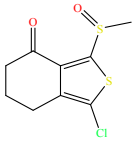	108	0.40	117	0.39
3	AC39661	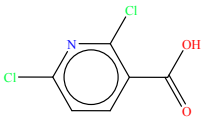	1518	0.36	3236	0.32
4	MAY00266	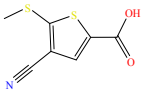	790	0.36	3091	0.29
5	RF03759	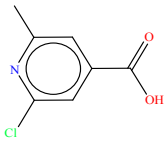	1777	0.35	1725	0.35
6	CC22101	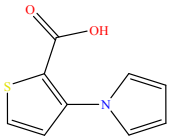	580	0.35	617	0.35
7	KM01280	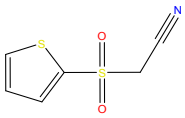	2571	0.33	613	0.41
8	CD11333	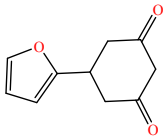	826	0.33	1926	0.29
9	SEW05732	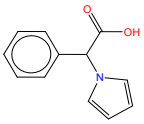	399	0.32	272	0.33
10	KM05951	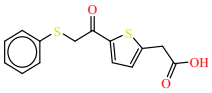	209	0.27	372	0.25
11	AC40357	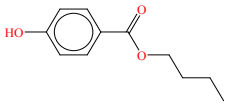	2369	0.26	NA	-
12	BTB10184	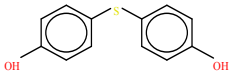	2245	0.25	2228	0.25

13	CC14901	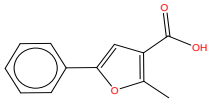	3924	0.23	2681	0.24

The IC_{50} was determined using a FRET-based assay on human or porcine RNase L. Ligand efficiency was calculated using the formula: LE = 1.4 × (-LogIC_{50}) /HAC. HAC is the number of heavy atoms (or non-hydrogen atoms). NA, not active.

Table S2. The potency of AC40357 derivatives against human (H-) and porcine (P-) RNase L

Compounds	2D-Structure	IC_{50} (μM) H-RNase L	IC_{50} (μM) P-RNase L
Phloretin	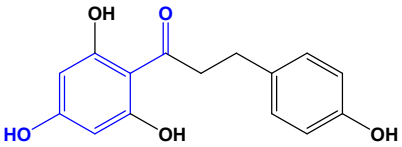	883	Not active
Liquiritin	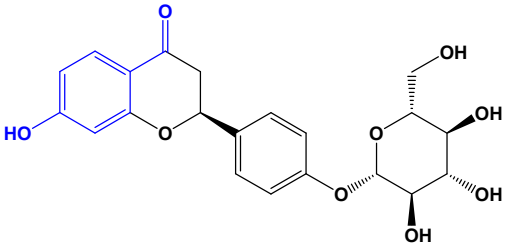	Not active	Not active
Myricetin	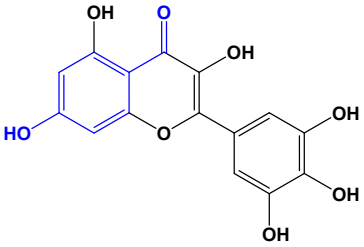	264	173
Hyperoside	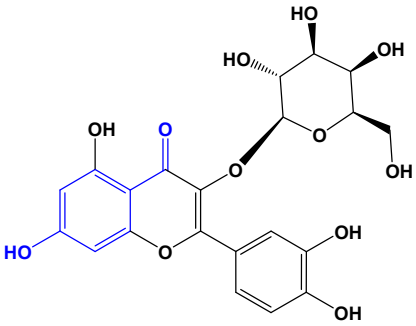	1.63	1.26

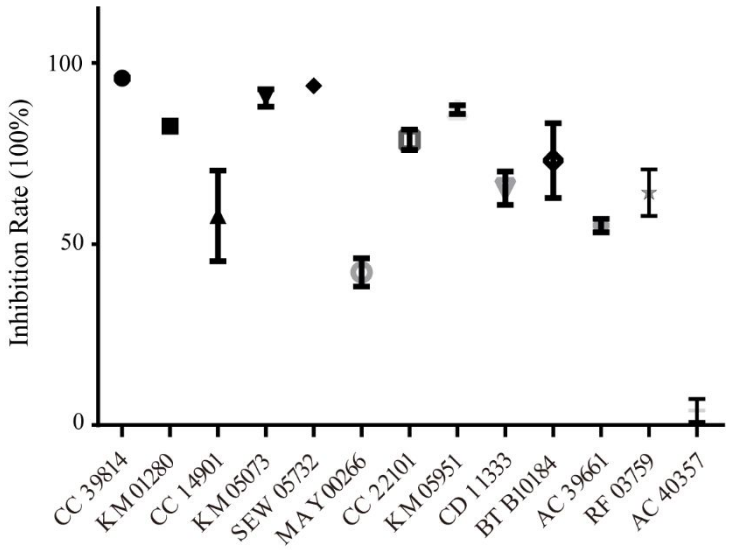

Figure S1. The inhibition rates of several fragments against P-RNase L.

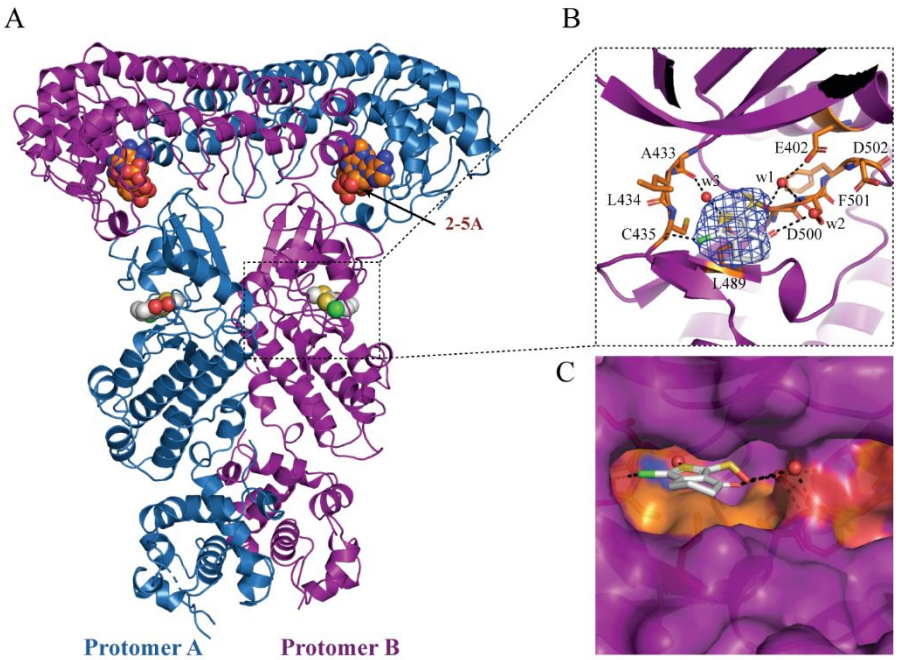

Figure S2. Co-crystal structure of the dimeric P-RNase L in complex with the fragment KM05073. (A) The dimer structure of P-RNase L in complex with 2-5A and KM05073. KM05073 bind to the PK domain in both protomers. (B) Stick model of KM05073 in P-RNase L, where the 2Fo-Fc density map of KM05073 is shown as blue mesh and contoured at 1 σ. Hydrogen bonds are shown as dotted black lines, and water molecules as red spheres. (C) The surface model KM05073 in P-RNase L.

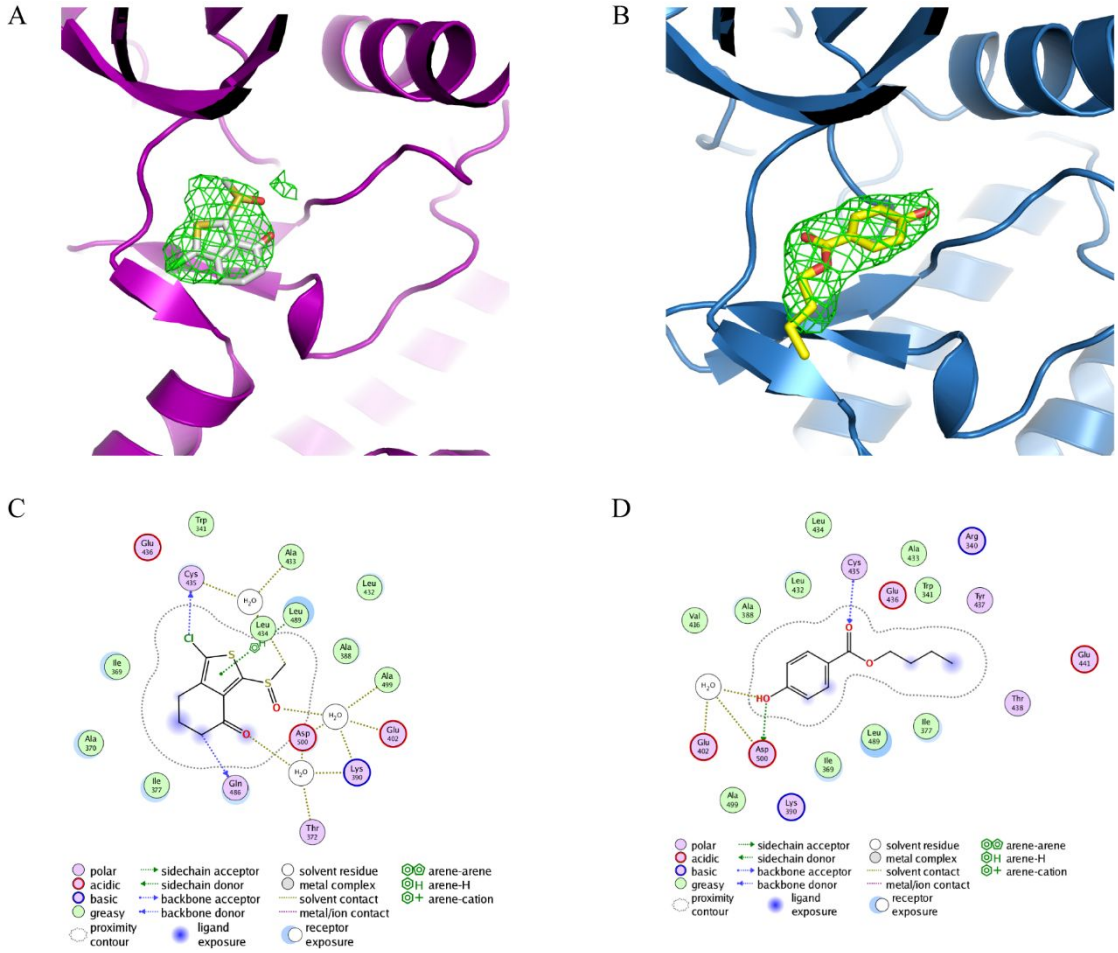

Figure S3. The Fo-Fc electron density omit map of fragments and the 2D Ligand interaction diagrams. The Fo-Fc density maps of KM05073 (A) and AC40357 (B) before refinement were shown. Interactions between RNase L and KM05073 (C) or AC40357 (D) were calculated using the MOE software.

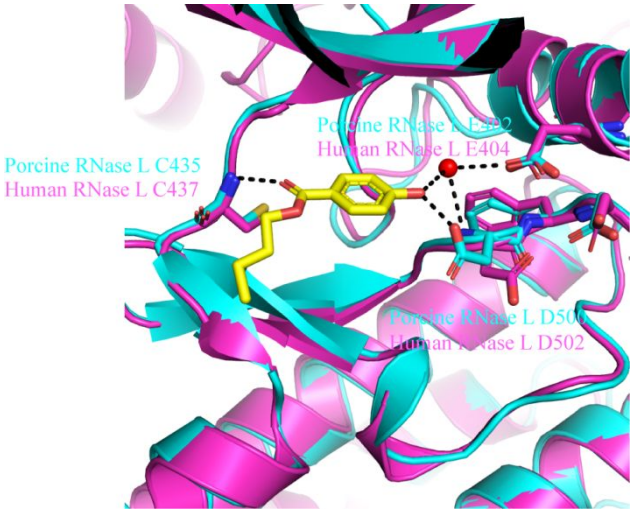

Figure S4. Critical residues in the fragments binding pocket are conserved in both human and porcine RNase L. The compound in yellow is AC40357. The ribbon structure in magenta is H-RNase L (PDB 4OAV) with ADP and Mg^{2+} removed and the structure in cyan is P-RNase L in complex with AC40357 (PDB 7DTS). The binding of AC40357 has caused swing of the side chain of D500 of P-RNase L.

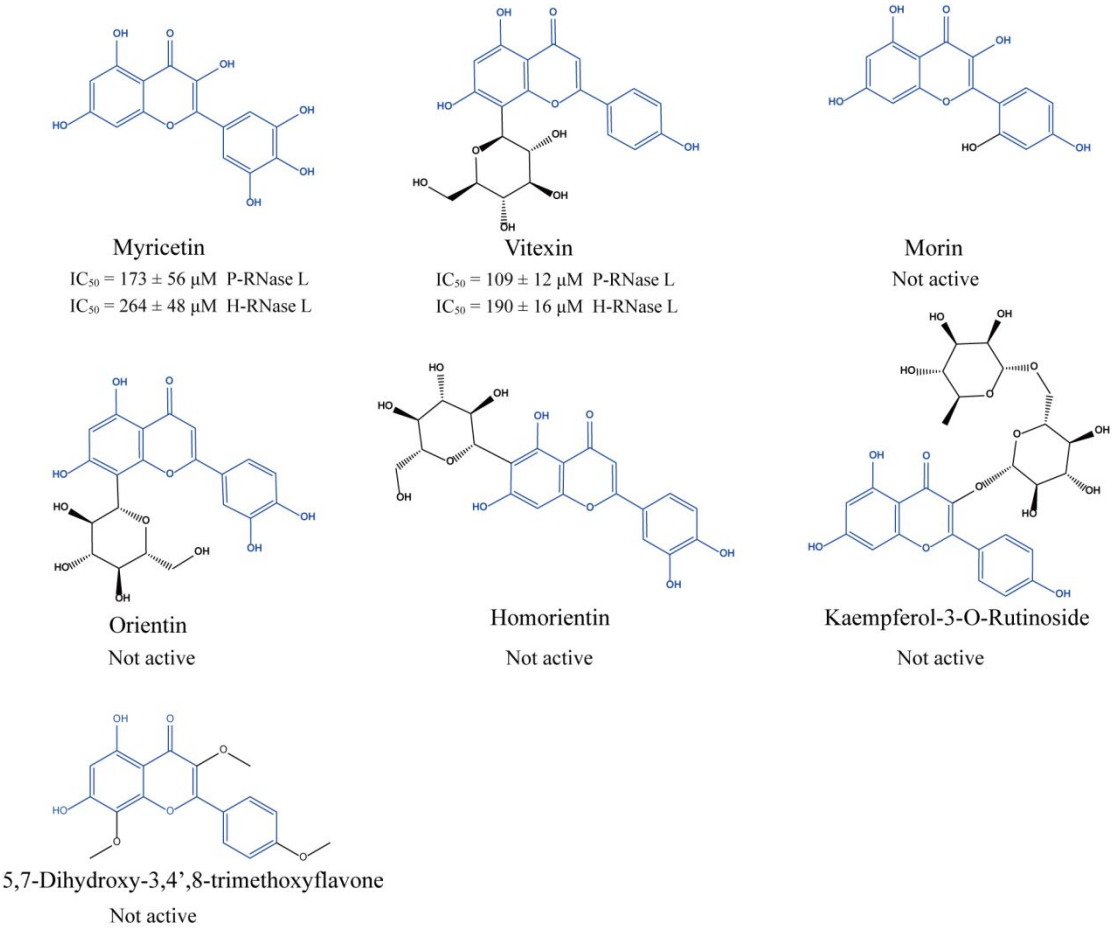

Figure S5. The potency of six myricetin derivatives against human and porcine RNase L. IC_{50} values represent the mean ± SEM of three inhibition profiles. Compounds not active for either

H- or P-RNase L were labelled with Not active.

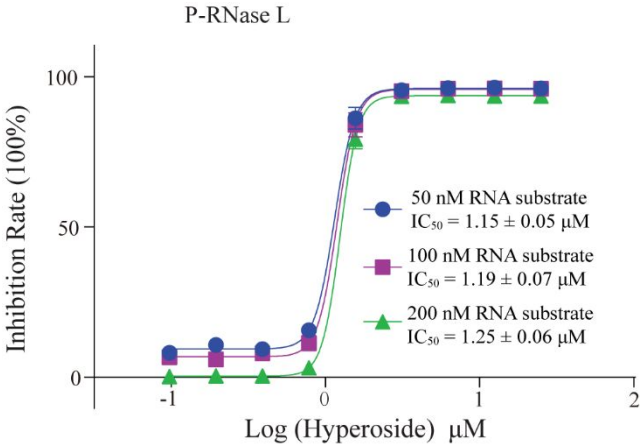

Figure S6. RNA substrate concentration does not affect the inhibition of hyperoside against P-RNase L. IC_{50} values represent the mean ± SEM of three inhibition profiles.

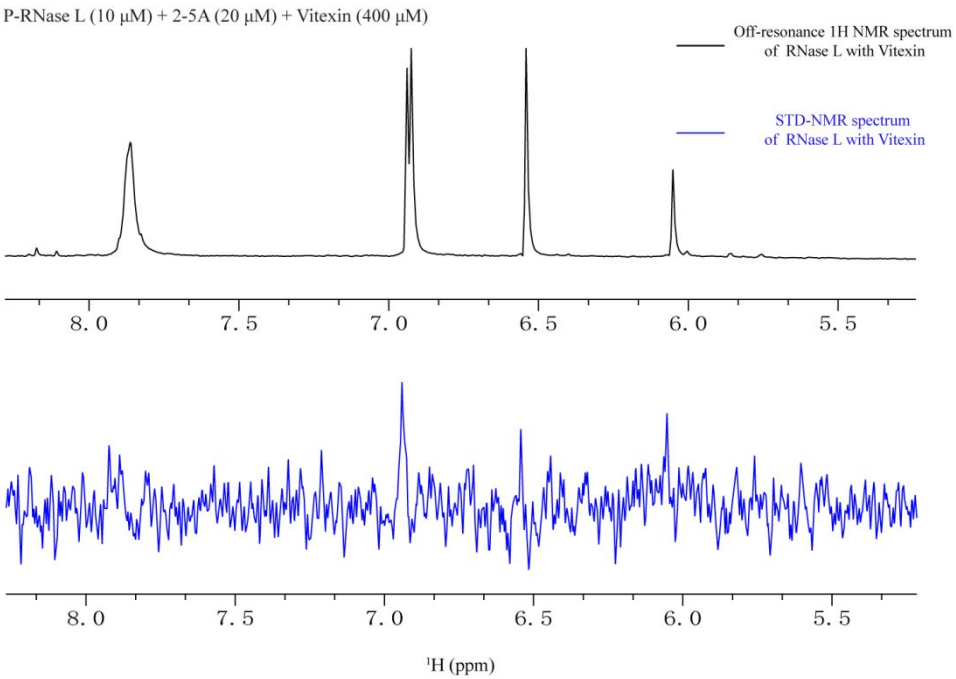

Figure S7. STD-NMR showed that vitexin directly binds to P-RNase L.

.

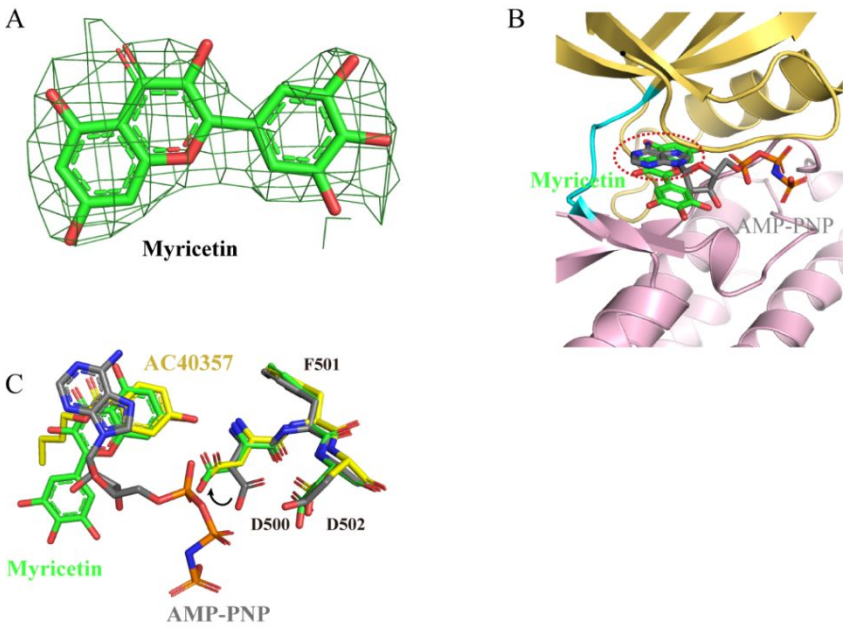

Figure S8. The density map of myricetin in the co-crystal structure with P-RNase L and structural comparison. (A) The Fc-Fo density map of myricetin (PDB 7ELW) before refinement was shown as forest green mesh and contoured at 3.0 σ. (B) Ribbon plot of P-RNase L showing the superposition of AMP-PNP (PDB 4O1P; gray stick model; nitrogen atoms in blue) and myricetin (green, in this study) on porcine RNase L (PDB 7ELW). (C) Compared with the structure of RNase L/AMP-PNP (PDB 4O1P), myricetin (PDB 7ELW) and AC40357 (PDB 7DTS) in the same binding pocket both induced slight swing of the side chain of D500.

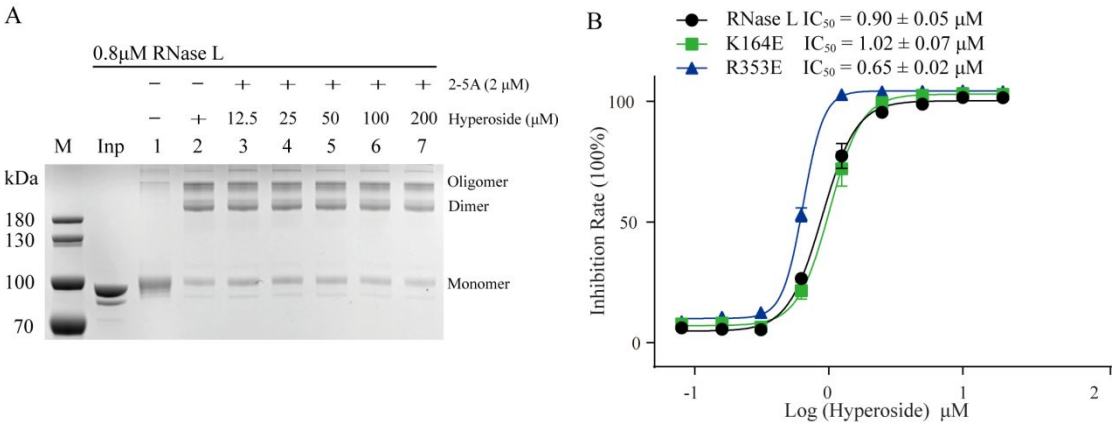

Figure S9. The potency of hyperoside was not affected by 2-5A binding. (A) Hyperoside did not affect 2-5A induced P-RNase L oligomerization. (B) Hyperoside displayed similar inhibitory activity against wt-P-RNase L and its two mutants (K164E and R353E).